Delayed contrast-enhanced computed tomography in patients with known or suspected cardiac sarcoidosis: a feasibility study

Tadao Aikawa, MD; Noriko Oyama-Manabe, MD, PhD; Masanao Naya, MD, PhD; Hiroshi Ohira, MD, PhD; Ayako Sugimoto, MD; Ichizo Tsujino, MD, PhD; Masahiko Obara, MD; Osamu Manabe, MD, PhD; Kohsuke Kudo, MD, PhD; Hiroyuki Tsutsui, MD, PhD; Nagara Tamaki, MD, PhD

Department of Cardiovascular Medicine (T.A., M.N., M.O.), Department of Diagnostic and Interventional Radiology (N.O-M., K.K.), First Department of Medicine (H.O., A.S., I.T.), and Department of Nuclear Medicine (O.M., N.T.), Hokkaido University Graduate School of Medicine, Kita-15, Nishi-7, Kita-ku, Sapporo 060-8638, Japan; Department of Cardiovascular Medicine, Kyushu University, 3-1-1, Maidashi, Higashi-ku, Fukuoka, 812-8582, Japan (H.T.)

Correspondence to: Noriko Oyama-Manabe
Department of Diagnostic and Interventional Radiology, Hokkaido University Hospital, Kita-15, Nishi-7, Kita-ku, Sapporo 060-8638, Japan
Tel.: +81-11-706-5977
Fax: +81-11-706-7876
E-mail: norikooyama@med.hokudai.ac.jp

Abstract

Objectives: To evaluate the diagnostic value of delayed contrast-enhanced computed tomography (DE-CT) for cardiac sarcoidosis (CS) in patients with or without implantable devices, including a quantitative comparison with late gadolinium enhancement cardiac magnetic resonance (LGE-CMR).

Methods: Twenty-four patients (mean age, 64 ± 9 years; 17 women) with known or suspected CS underwent retrospective electrocardiogram-gated DE-CT at 80 kV with knowledge-based iterative model reconstruction. Fourteen patients without implantable devices also underwent LGE-CMR, while 10 with pacemakers or implantable cardioverter-defibrillators did not. The presence of hyperenhanced myocardium was assessed visually and quantitatively using a 5-standard deviation threshold above the mean of remote myocardium.

Results: Inter-observer agreement for visual detection of hyperenhanced segments on DE-CT was excellent in patients with implantable devices and in those without ($\kappa = 0.91$ and $\kappa = 0.94$, respectively). Comparisons of the percent area of hyperenhanced myocardium between DE-CT and LGE-CMR on both per-patient and per-segment analyses showed good correlations ($r = 0.96$ and $r = 0.83$, respectively; $p < 0.001$). The sensitivity and specificity of DE-CT for the diagnosis of CS were 94% and 33%, respectively.

Conclusions: The extent of hyperenhanced lesion with DE-CT showed good agreement with LGE-CMR results. DE-CT showed high sensitivity for detecting CS and may be useful particularly in patients with contraindications to CMR.

Keywords

Cardiac sarcoidosis; Cardiac CT; Delayed enhancement; Myocardium; Iterative reconstruction.

Key points

- Delayed contrast-enhanced CT (DE-CT) can be applied to patients with implantable devices.
- DE-CT can detect cardiac sarcoidosis (CS) lesions similarly to cardiac MRI.
- DE-CT shows high sensitivity for detecting CS.
- DE-CT may be useful particularly in patients with contraindications to cardiac MRI.

Abbreviations

- CI = confidence interval
- CMR = cardiac magnetic resonance
- CNR = contrast-to-noise ratio
- CS = cardiac sarcoidosis
- DE-CT = delayed contrast-enhanced computed tomography
- JSSOG = Japanese Society of Sarcoidosis and other Granulomatous Disorder
- LGE = late gadolinium enhancement
- SD = standard deviation
- SNR = signal-to-noise ratio

Introduction

Sarcoidosis is a systemic granulomatous disease of unknown aetiology [1]. Although cardiac sarcoidosis (CS) is encountered in only 2%–5% of patients with systemic sarcoidosis [2, 3], the presence of CS is an important prognostic factor in patients with the disease [4]. In patients with systemic sarcoidosis, late gadolinium enhancement (LGE) cardiac magnetic resonance (CMR) allows noninvasive assessment of CS [5, 6]. Furthermore, the presence and extent of LGE have been reported to predict adverse cardiac events in patients with systemic sarcoidosis [6-9]. However, the applicability of LGE-CMR for CS is limited in patients with pacemakers or implantable cardioverter-defibrillators.

Several studies have reported that delayed contrast-enhanced computed tomography (DE-CT) imaging showed good agreement with LGE-CMR in patients with coronary artery disease [10-12], hypertrophic cardiomyopathy [13], and cardiac amyloidosis [14] because iodinated contrast material accumulates in the myocardial scar in a manner similar to that of gadolinium chelates [11, 15]. Furthermore, DE-CT can be applied to patients with implantable devices [16, 17]. However, the clinical utility of DE-CT for evaluation of CS and its image quality in patients with and without implantable devices have not been reported. DE-CT may be helpful as part of a comprehensive program for the screening or monitoring of sarcoidosis including cardiac involvements even in patients with implantable devices. Thus, the aim of study was to evaluate the diagnostic value of DE-CT for CS in patients with or

without implantable devices, including a quantitative comparison with the extent of CS as assessed by LGE-CMR.

Materials and methods

Study patients

This study was a retrospective evaluation of the clinical records of patients with known or suspected CS who underwent DE-CT at our hospital. All DE-CT examinations were performed in patients referred by their physicians for clinically indicated contrast-enhanced CT. The main purpose of performing contrast-enhanced CT in this population was for systemic evaluation for the clinical assessment of sarcoidosis and identification of appropriate sites for diagnostic biopsy in patients without pathological confirmation. The study was approved by the institutional review board with a waiver of the need for written informed consent.

In total, 35 consecutive patients were referred for DE-CT between May 2015 and August 2016 for at least 1 of the following indications: known CS, known extracardiac sarcoidosis, new-onset atrioventricular block, new-onset ventricular tachycardia, or left ventricular aneurysm. Of these patients, patients who had a history of previous myocardial infarction (n = 4) or other known cardiomyopathy (n = 6) and who did not undergo a standard clinical assessment of CS in our hospital (n = 1) were excluded. Thus, a total of 24 patients (mean age, 64 ± 9 years; 17 women, 7 men) were included in this analysis. Of these 24 patients, 14 patients without any implantable devices also underwent LGE-CMR (median interval, 4 days; range 1–32 days), and no changes in medication or clinical events occurred between the two

examinations. The order of referring patients for DE-CT and LGE-CMR did not influence the selection of patients because both modalities were simultaneously ordered as part of the clinical assessment of CS. The remaining 10 patients with implantable devices (8 with a pacemaker, and 2 with an implantable cardioverter-defibrillator) did not undergo LGE-CMR. After the DE-CT scan, each patient also underwent a standard clinical assessment, as previously reported [5, 18], for the diagnosis of CS based on the 2015 Japanese Society of Sarcoidosis and other Granulomatous Disorders (JSSOG) criteria (Table 1), which was assessed separately from the DE-CT results. In addition, patients with coronary risk factors underwent stress myocardial perfusion imaging, CT coronary angiography, or invasive coronary angiography to exclude significant coronary artery disease.

DE-CT image acquisition

All patients underwent an initial whole-body contrast-enhanced CT scan after administration of 600 mg iodine/kg of iodinated contrast medium (370 mg iodine/mL) for evaluation of systemic sarcoidosis. Cardiac DE-CT was performed 15 minutes after the contrast injection as previously suggested [10], using a retrospectively electrocardiogram (ECG)-gated cardiac 256-row detector CT (Brilliance iCT Elite, Philips Healthcare, Cleveland, OH) without additional injection of contrast medium or beta-blocker. DE-CT parameters were as follows: detector configuration, 128 × 0.625 mm; slice thickness, 0.625 mm; rotation time, 0.27 s;

helical pitch, 0.16; tube voltage, 80 kV; and tube current–time products, 800–1200 mAs (range) with ECG tube current modulation. The acquisition data were reconstructed at 75% of the RR interval using a knowledge-based iterative model reconstruction algorithm (IMR, Philips Healthcare) [19] (Fig. 1).

Radiation dose estimation

The effective radiation doses of whole-body CT and DE-CT were derived from multiplying the dose-length product for each scan by a conversion factor of 0.015 mSv × $(mGy \times cm)^{-1}$ for the whole-body and by a conversion factor of 0.014 mSv × $(mGy \times cm)^{-1}$ for the chest [20, 21].

LGE-CMR image acquisition

CMR was performed following established protocols using a 1.5-T whole-body scanner (Achieva, Philips Medical Systems, Best, The Netherlands) with a 5-channel phased-array cardiac coil (n = 8) [22] or a 3-T whole-body scanner (Achieva Tx, Philips Medical Systems) with a 32-channel phased-array receiver torso-cardiac coil (n = 6) [23] in accordance with the Society for Cardiovascular Magnetic Resonance guidelines [24]. LGE-CMR imaging was performed 10–15 minutes after administration of Gd-DTPA (0.1 mmol/kg, Magnevist; Berlex Laboratories, Wayne, NJ) with an inversion-recovery prepared, 3-dimensional fast field echo

pulse sequence. The entire volume of the heart was covered in 5 mm slice thickness with no gap.

Data analysis

All DE-CT and LGE-CMR images were analysed using commercially available software (Ziostation2, Ziosoft Inc., Tokyo, Japan). The short axis images for qualitative and quantitative analysis were reconstructed at 5-mm slice thickness. The software automatically generated the 16 segments (excluding the apex) of the American Heart Association 17-segment model, using a vertical line from the centre of the left ventricle to the interventricular septum. Two observers (with 2 and 18 years of experience in cardiac imaging, respectively) who were blinded to the clinical history independently assessed the quality of the DE-CT images (good, sufficient, and non-assessable); they also evaluated the presence (present, absent, and non-assessable) and transmularity (subendocardial, midwall, subepicardial, and transmural) of hyperenhanced myocardium in each segment on the DE-CT and LGE-CMR images. The presence of hyperenhancement in the right ventricular wall was also visually evaluated. After initial evaluation, any inter-observer disagreements were resolved by consensus.

Quantitative analysis of DE-CT and LGE-CMR was also performed using the same software (Ziostation2, Ziosoft Inc.), which automatically determined hyperenhanced

myocardium as that exhibiting CT attenuation or CMR signal intensity above a predetermined threshold. The extent of hyperenhanced myocardium was quantified as the percentage area of myocardium with CT attenuation or CMR signal intensity ≥ 5 standard deviations (SDs) above the mean for CT attenuation or CMR signal intensity in the remote myocardium (Fig. 2) [7, 25]. The contrast-to-noise ratio (CNR) was calculated as the difference in CT attenuation or CMR signal intensity between the hyperenhanced and remote myocardium, divided by the SD value in the remote myocardium [12]. For these measurements, a single circular region of interest (more than 10 mm^2) was placed over the hyperenhanced or remote myocardium.

$$CNR = \frac{mean\ of\ the\ hyperenhanced\ myocardium - mean\ of\ the\ remote\ myocardium}{SD\ of\ the\ remote\ myocardium}$$

The signal-to-noise ratio (SNR) was calculated as the mean attenuation or signal intensity of the remote myocardium divided by the SD value in the remote myocardium [12].

$$SNR = \frac{mean\ of\ the\ remote\ myocardium}{SD\ of\ the\ remote\ myocardium}$$

Statistical analysis

Continuous variables are presented as the mean ± SD or median and interquartile range, as appropriate. Categorical variables are presented as absolute numbers or percentages. The Shapiro–Wilk test was applied to evaluate the distribution of data. Inter-observer agreements regarding visual assessments of DE-CT was evaluated by Cohen's κ-statistics with the

following interpretation of κ values: >0.80, excellent agreement; 0.61–0.80, good; 0.41–0.60, moderate; 0.21–0.40, fair; <0.20, poor agreement [26]. The difference in DE-CT image quality between patients with and without implantable devices was compared using the Mann–Whitney *U* test. Differences in quantitative parameters on DE-CT between patients with and without implantable devices were compared using an unpaired *t*-test after normality testing. Correlation and agreement in the quantitative extent of hyperenhanced myocardium between DE-CT and LGE-CMR were evaluated by linear regression analysis and Bland-Altman analysis on a per-patient and per-segment basis. Differences in quantitative parameters (SNR and CNR) between DE-CT and LGE-CMR were compared using a paired *t*-test after normality testing. The diagnostic values of DE-CT and LGE-CMR for identifying JSSOG criteria-based CS were expressed as sensitivity, specificity, positive predictive value, and negative predictive value. In all tests, statistical significance was considered at $p < 0.05$. All statistical analyses were performed using JMP Pro 12.0.1 (SAS Institute Inc., Cary, NC).

Results

Patient characteristics are shown in Table 2. Among the 24 patients, 10 patients had known CS prior to DE-CT, and 8 patients with suspected CS were newly diagnosed with CS: 2 with histological diagnosis and 6 with clinical diagnosis. The remaining 6 patients did not meet the JSSOG criteria, and none of them showed abnormal uptake of ^{18}F-fluorodeoxyglucose in the myocardium.

DE-CT image quality and assessability in patients with or without implantable devices

In the 14 patients without implantable devices, a total of 224 segments on DE-CT were assessable; 167 (75%) were good quality, and 57 (25%) were of sufficient quality. Among the 10 patients with implantable devices, 9 had at least 1 non-assessable segment on DE-CT, mainly because of the artifacts from their device leads in the septum (Fig. 3), while 1 patient showed no such artifacts. In the 160 segments on DE-CT of the 10 patients with implantable devices, 101 (63%) were of good quality, 26 (16%) were of sufficient quality, and 33 segments (21%) including 18 septal segments were classified as non-assessable ($p < 0.001$ vs. patients without implantable devices).

In 14 patients who underwent both DE-CT and LGE-CMR, there was no discrepancy in hyperenhancement between them; 13 patients having hyperenhancement on DE-CT also presented hyperenhanced myocardium on LGE-CMR, and 1 patient had no

hyperenhancement on both modalities. Hyperenhanced myocardium was visually identified on DE-CT in 8 patients with implantable devices. An average of 5.3 ± 3.9 segments showed hyperenhancement. The distribution of hyperenhanced myocardium on DE-CT is shown in Table 3. In the per-segment analysis, the inter-observer agreement for visual detection of hyperenhanced segments on DE-CT was excellent in patients without implantable devices (κ = 0.94; 95% confidence interval [CI], 0.90–0.99; $p < 0.001$) and in patients with implantable devices (κ = 0.91; 95% CI, 0.85–0.97; $p < 0.001$). Both the SNR and CNR on DE-CT did not differ significantly between patients with and without implantable devices (p = 0.72 and p = 0.17, respectively) (Table 4).

Quantitative comparison between DE-CT and LGE-CMR in patients without implantable devices

The mean extent of hyperenhanced myocardium on DE-CT was 11.0% ± 10.9% (range, 0%–31.3%), which was similar to that on LGE-CMR (11.8% ± 10.7%; range, 0%–32.8%). Quantitative comparisons of the extent of hyperenhanced myocardium between DE-CT and LGE-CMR on both per-patient and per-segment analyses showed good correlation (r = 0.96 and r = 0.83, respectively; both $p < 0.001$) and small mean differences (−0.9% ± 3.0% and −1.0% ± 10.9%, respectively) (Fig. 4). The SNR on DE-CT was significantly higher than that on LGE-CMR (14.2 ± 4.8 vs. 7.0 ± 4.6, $p < 0.001$). In the 13 patients with hyperenhancement

on both modalities, the CNR on DE-CT did not significantly differ from that on LGE-CMR (7.3 ± 2.5 vs. 7.5 ± 3.2, $p = 0.88$). Hyperenhancement on the right ventricular myocardium was identified on LGE-CMR in 6 patients, while none of them had detectable hyperenhancement on DE-CT because of insufficient wall thickness of the right ventricle.

Diagnostic value of DE-CT for CS

Comparisons between DE-CT and LGE-CMR findings and clinical diagnosis based on the JSSOG criteria are shown in Table 5. In the 4 patients with false-positive DE-CT results, 3 patients without implantable devices also presented hyperenhancement on LGE-CMR, and 1 patient with an implantable cardioverter-defibrillator who had left ventricular aneurysm of unknown aetiology was not proven to have extracardiac sarcoidosis. One patient with a false-negative DE-CT result had known CS and a pacemaker. The overall diagnostic values of DE-CT for identifying JSSOG criteria-based CS were as follows: the sensitivity, specificity, positive predictive value, and negative predictive value were 94% (95% CI, 74%–99%), 33% (95% CI, 10%–70%), 81% (95% CI, 60%–92%), and 67% (95% CI, 21%–94%), respectively. In 14 patients without implantable devices, the diagnostic values of LGE-CMR were equal to those of DE-CT and were as follows: the sensitivity, specificity, positive predictive value, and negative predictive value were 100% (95% CI, 72%–100%), 25% (95% CI, 5%–70%), 77% (95% CI, 50%–92%), and 100% (95% CI, 21%–100%), respectively.

DE-CT radiation dose

The mean dose-length product was 398.6 ± 78.6 mGy·cm (range, 220.2–579.8 mGy·cm). The estimated radiation dose of DE-CT was 5.6 ± 1.1 mSv (range, 3.1–8.1 mSv), which was approximately half that of the whole-body CT scan without DE-CT (mean dose, 11.5 ± 4.1 mSV; range, 6.2–18.9 mSv).

Discussion

This study shows that DE-CT had sufficient image quality to allow the assessment of hyperenhanced myocardium in patients with or without implantable devices. DE-CT delineated the extent of CS with accuracy comparable to that of LGE-CMR. DE-CT had high sensitivity for the diagnosis of CS, suggesting that DE-CT may be appropriate for screening and monitoring of CS, particularly in patients with contraindications to CMR.

The present study demonstrated that non-assessable segments were limited in patients with or without implantable devices (21% and 0%, respectively), and that the inter-observer agreement in visual assessments for DE-CT was excellent regardless of the presence or absence of implantable devices. These findings suggest that implantable devices had a limited impact on the quality of DE-CT images. The degree to which DE-CT images could be assessed in patients with implantable devices was concordant with previous reports of metal artifacts arising from a device lead impairing the image quality for DE-CT of the septum [16, 17]. We used the knowledge-based iterative model reconstruction algorithm [19], which is a recently developed full-iterative reconstruction algorithm for image noise reduction. A previous study suggested that CT images that undergo full-iterative reconstruction show reduced image noise and provide better image quality than those obtained with filtered back-projection or hybrid iterative reconstruction [27]. In addition, several reconstruction algorithms for reducing metal artifacts arising from implantable devices on CT images have

been proposed [28, 29]; development of such a reconstruction algorithm has the potential to further improve the quality of images obtained using DE-CT in patients with implantable devices.

In the present study, the extent of hyperenhanced myocardium on DE-CT in patients with CS was in good agreement with that on LGE-CMR. This finding is concordant with the results of previous DE-CT studies performed in patients with myocardial infarction [10-12]. To our knowledge, this is the first quantitative comparison of the extent of hyperenhancement between DE-CT and LGE-CMR in patients with CS. LGE-CMR is one of the major criteria in the currently proposed guidelines for diagnosis of CS published in 2015 by the JSSOG and in 2014 by the Heart Rhythm Society [30]. The presence of hyperenhancement on LGE-CMR can identify not only cardiac involvement in sarcoidosis but also patients at high risk for adverse cardiac events [8, 9]. Furthermore, the extent of hyperenhanced myocardium on LGE-CMR has been demonstrated to predict adverse cardiac events in patients with CS [7, 25]. While LGE-CMR can evaluate only myocardium, contrast-enhanced CT can evaluate the whole-body and myocardium on delayed phase. DE-CT has the potential to detect myocardial fibrosis due to CS as part of evaluation for systemic sarcoidosis.

The sensitivity of DE-CT for identifying JSSOG criteria-based CS was high, while the specificity was relatively low despite the exclusion of patients with previous myocardial infarction or other known cardiomyopathy. Regarding this point, Ohira *et al.* reported that

LGE-CMR can detect damaged myocardium in CS patients without active inflammation as detected by ^{18}F-fluorodeoxyglucose positron emission tomography [5], suggesting that DE-CT may also detect potential CS lesions not fulfilling the JSSOG criteria due to low disease activity with fibrosis. In the present study, the 3 patients with false-positive DE-CT results all showed hyperenhancement on LGE-CMR. Therefore, DE-CT may be feasible for screening for and ruling out CS, whereas the role of DE-CT at different stages of the disease process requires further investigation.

LGE-CMR is well established for the assessment of CS. However, LGE-CMR cannot be performed in patients with CMR-incompatible devices. This is a major problem for patients with CS, given that they often have complications, such as conduction abnormalities or life-threatening ventricular arrhythmias requiring pacemakers or implantable cardioverter-defibrillators [18, 31]. In contrast, DE-CT can be performed in patients with any type of implantable devices without a need to interrogate or reprogram the devices, and in a shorter scan time than with CMR, which are important advantages in a clinical setting. However, in contrast to LGE-CMR, DE-CT requires radiation exposure and nephrotoxic contrast material. To mitigate this, we used a relatively low tube voltage (80 kV) for reduction of radiation exposure. Further, compared with LGE-CMR, DE-CT may be more difficult to assess in patients with non-ischemic cardiomyopathy [32]. Although not the primary focus of the study, we found that DE-CT could not detect right ventricular

involvement in CS due to insufficient wall thickness of the right ventricle. This might be a disadvantage of DE-CT because LGE-CMR enables reliable detection of right ventricular involvement in CS [33].

Earlier DE-CT studies quantified hyperenhanced myocardium using manual planimetry in each slice [11, 12]. Although manual planimetry is a reasonable approach for assessment of focal hyperenhancement, such as infarcted myocardium, the method is somewhat arbitrary and is unsuitable for patchy CS lesions. Therefore, in the present study, we used the 5 SD technique, which is widely used in LGE-CMR studies [7, 25], to delineate the hyperenhanced myocardium seen on DE-CT in patients with CS.

The current study has several limitations. First, we did not perform LGE-CMR in patients with implantable devices, and this may affect the diagnosis of CS in these patients. However, 7 of 10 patients with implantable devices had already known CS, and all of them showed positive DE-CT results. One patient was newly diagnosed as having CS even without CMR. In addition, although we did not provide a correlation between DE-CT and LGE-CMR in patients with implantable devices, the patients without implantable devices had good agreement between DE-CT and LGE-CMR findings. Second, the small sample size resulted in wide confidence intervals of the diagnostic value of DE-CT. A further prospective study is needed to evaluate the diagnostic value of DE-CT for CS. Third, recent studies have reported the feasibility of prospective ECG-gated scanning for a further decrease in the radiation dose

[34]. However, prospective ECG-gated scanning is known to be less suitable at high heart rates and is reported to have a lower SNR and CNR when compared with retrospective ECG-gated scanning [35]. In the present study, retrospective ECG-gated scanning with tube current modulation was successfully applied for all cases without altering the heart rate, especially for patients with atrial fibrillation, heart rate of 70 beats/min or higher, or infrequent pacing. Prospective trials to optimize DE-CT scan protocols are warranted.

In conclusion, DE-CT can detect CS lesions with similar efficacy to LGE-CMR and provides diagnostic information even in patients with implantable devices. DE-CT showed high sensitivity for detection of CS and may be useful particularly in patients with contraindications to CMR.

References

1 Iannuzzi MC, Rybicki BA, Teirstein AS (2007) Sarcoidosis. N Engl J Med 357:2153-2165

2 Baughman RP, Teirstein AS, Judson MA et al (2001) Clinical characteristics of patients in a case control study of sarcoidosis. Am J Respir Crit Care Med 164:1885-1889

3 Valeyre D, Prasse A, Nunes H, Uzunhan Y, Brillet PY, Muller-Quernheim J (2014) Sarcoidosis. Lancet 383:1155-1167

4 Blankstein R, Osborne M, Naya M et al (2014) Cardiac positron emission tomography enhances prognostic assessments of patients with suspected cardiac sarcoidosis. J Am Coll Cardiol 63:329-336

5 Ohira H, Birnie DH, Pena E et al (2016) Comparison of (18)F-fluorodeoxyglucose positron emission tomography (FDG PET) and cardiac magnetic resonance (CMR) in corticosteroid-naive patients with conduction system disease due to cardiac sarcoidosis. Eur J Nucl Med Mol Imaging 43:259-269

6 Patel MR, Cawley PJ, Heitner JF et al (2009) Detection of myocardial damage in patients with sarcoidosis. Circulation 120:1969-1977

7 Ise T, Hasegawa T, Morita Y et al (2014) Extensive late gadolinium enhancement on cardiovascular magnetic resonance predicts adverse outcomes and lack of

improvement in LV function after steroid therapy in cardiac sarcoidosis. Heart 100:1165-1172

8 Coleman GC, Shaw PW, Balfour PC, Jr. et al (2016) Prognostic value of myocardial scarring on CMR in patients with cardiac sarcoidosis: a systematic review and meta-analysis. JACC Cardiovasc Imaging. DOI: 10.1016/j.jcmg.2016.05.009

9 Hulten E, Agarwal V, Cahill M et al (2016) Presence of late gadolinium enhancement by cardiac magnetic resonance among patients with suspected cardiac sarcoidosis is associated with adverse cardiovascular prognosis: a systematic review and meta-analysis. Circ Cardiovasc Imaging 9:e005001

10 Mahnken AH, Koos R, Katoh M et al (2005) Assessment of myocardial viability in reperfused acute myocardial infarction using 16-slice computed tomography in comparison to magnetic resonance imaging. J Am Coll Cardiol 45:2042-2047

11 Gerber BL, Belge B, Legros GJ et al (2006) Characterization of acute and chronic myocardial infarcts by multidetector computed tomography: comparison with contrast-enhanced magnetic resonance. Circulation 113:823-833

12 Nieman K, Shapiro MD, Ferencik M et al (2008) Reperfused myocardial infarction: contrast-enhanced 64-Section CT in comparison to MR imaging. Radiology 247:49-56

13 Zhao L, Ma X, Delano MC et al (2013) Assessment of myocardial fibrosis and coronary arteries in hypertrophic cardiomyopathy using combined arterial and delayed enhanced CT: comparison with MR and coronary angiography. Eur Radiol 23:1034-1043

14 Deux JF, Mihalache CI, Legou F et al (2015) Noninvasive detection of cardiac amyloidosis using delayed enhanced MDCT: a pilot study. Eur Radiol 25:2291-2297

15 Lardo AC, Cordeiro MA, Silva C et al (2006) Contrast-enhanced multidetector computed tomography viability imaging after myocardial infarction: characterization of myocyte death, microvascular obstruction, and chronic scar. Circulation 113:394-404

16 Esposito A, Palmisano A, Antunes S et al (2016) Cardiac CT With Delayed Enhancement in the Characterization of Ventricular Tachycardia Structural Substrate: Relationship Between CT-Segmented Scar and Electro-Anatomic Mapping. JACC Cardiovasc Imaging 9:822-832

17 Shiozaki AA, Senra T, Arteaga E et al (2013) Myocardial fibrosis detected by cardiac CT predicts ventricular fibrillation/ventricular tachycardia events in patients with hypertrophic cardiomyopathy. J Cardiovasc Comput Tomogr 7:173-181

18 Manabe O, Ohira H, Yoshinaga K et al (2013) Elevated (18)F-fluorodeoxyglucose uptake in the interventricular septum is associated with atrioventricular block in

patients with suspected cardiac involvement sarcoidosis. Eur J Nucl Med Mol Imaging 40:1558-1566

19 Oda S, Utsunomiya D, Funama Y et al (2014) A knowledge-based iterative model reconstruction algorithm: can super-low-dose cardiac CT be applicable in clinical settings? Acad Radiol 21:104-110

20 Hausleiter J, Meyer T, Hermann F, et al. (2009) Estimated radiation dose associated with cardiac CT angiography. JAMA 301:500-507

21 Christner JA, Kofler JM, McCollough CH (2010) Estimating effective dose for CT using dose-length product compared with using organ doses: consequences of adopting International Commission on Radiological Protection publication 103 or dual-energy scanning. AJR Am J Roentgenol 194:881-889

22 Sato T, Tsujino I, Ohira H et al (2013) Paradoxical interventricular septal motion as a major determinant of late gadolinium enhancement in ventricular insertion points in pulmonary hypertension. PLoS One 8:e66724

23 Oyama-Manabe N, Ishimori N, Sugimori H et al (2011) Identification and further differentiation of subendocardial and transmural myocardial infarction by fast strain-encoded (SENC) magnetic resonance imaging at 3.0 Tesla. Eur Radiol 21:2362-2368

24 Kramer CM, Barkhausen J, Flamm SD, Kim RJ, Nagel E (2013) Standardized cardiovascular magnetic resonance (CMR) protocols 2013 update. J Cardiovasc Magn Reson 15:91

25 Murtagh G, Laffin LJ, Beshai JF et al (2016) Prognosis of myocardial damage in sarcoidosis patients with preserved left ventricular ejection fraction: risk stratification using cardiovascular magnetic resonance. Circ Cardiovasc Imaging 9:e003738

26 Kundel HL, Polansky M (2003) Measurement of observer agreement. Radiology 228:303-308

27 Oda S, Weissman G, Vembar M, Weigold WG (2015) Cardiac CT for planning redo cardiac surgery: effect of knowledge-based iterative model reconstruction on image quality. Eur Radiol 25:58-64

28 Boas FE, Fleischmann D (2011) Evaluation of two iterative techniques for reducing metal artifacts in computed tomography. Radiology 259:894-902

29 Morsbach F, Bickelhaupt S, Wanner GA, Krauss A, Schmidt B, Alkadhi H (2013) Reduction of metal artifacts from hip prostheses on CT images of the pelvis: value of iterative reconstructions. Radiology 268:237-244

30 Birnie DH, Sauer WH, Bogun F et al (2014) HRS expert consensus statement on the diagnosis and management of arrhythmias associated with cardiac sarcoidosis. Heart Rhythm 11:1305-1323

31 Kandolin R, Lehtonen J, Airaksinen J et al (2015) Cardiac sarcoidosis: epidemiology, characteristics, and outcome over 25 years in a nationwide study. Circulation 131:624-632

32 Takaoka H, Funabashi N, Uehara M, Iida Y, Kobayashi Y (2017) Diagnostic accuracy of CT for the detection of left ventricular myocardial fibrosis in various myocardial diseases. Int J Cardiol 228:375-379

33 Fairbairn TA, Motwani M, Greenwood JP, Plein S (2012) CMR for the diagnosis of right heart disease. JACC Cardiovasc Imaging 5:227-229

34 Schuleri KH, George RT, Lardo AC (2009) Applications of cardiac multidetector CT beyond coronary angiography. Nat Rev Cardiol 6:699-710

35 Chang HJ, George RT, Schuleri KH et al (2009) Prospective electrocardiogram-gated delayed enhanced multidetector computed tomography accurately quantifies infarct size and reduces radiation exposure. JACC Cardiovasc Imaging 2:412-420

Table legends

Table 1. Japanese Society of Sarcoidosis and other Granulomatous Disorders (JSSOG) 2015 criteria for cardiac sarcoidosis.

1. Histological diagnosis group

   Cardiac sarcoidosis is confirmed when endomyocardial biopsy specimens demonstrate noncaseating epithelioid cell granulomas with a histological or clinical diagnosis of extracardiac sarcoidosis.

2. Clinical diagnosis group

   Cardiac sarcoidosis is confirmed when, although endomyocardial biopsy specimens do not demonstrate noncaseating epithelioid cell granulomas, extracardiac sarcoidosis is diagnosed histologically or clinically and the following diagnostic criteria are satisfied:

   a) Two or more of the five major criteria are met

   OR

   b) One of the five major criteria and two or more of the three minor criteria are met

   Major criteria

   1. Advanced atrioventricular block or sustained ventricular tachycardia
   2. Basal thinning of the interventricular septum or morphological abnormality (aneurysm, wall thinning, or wall thickening)
   3. Depressed ejection fraction (< 50%) or regional wall motion abnormality
   4. Abnormal uptake of ^{67}Ga or ^{18}F-fluorodeoxyglucose in the heart
   5. Late gadolinium enhancement on cardiac magnetic resonance

   Minor criteria

   1. Abnormal electrocardiographic findings: ventricular arrhythmias (non-sustained ventricular tachycardia or multifocal or frequent premature ventricular contractions), bundle branch block, axis deviation, or abnormal Q-waves
   2. Perfusion defects on nuclear imaging
   3. Endomyocardial biopsy: interstitial fibrosis or monocyte infiltration of moderate grade

Adapted Ohira et al. [5] to the JSSOG 2015 criteria

Table 2. Patient characteristics

	All patients (n = 24)	Without implantable devices (n = 14)	With implantable devices (n = 10)
Age (y)	64 ± 9	62 ± 10	67 ± 7
Women	17 (71)	9 (64)	8 (80)
Body mass index (kg/m^2)	22.1 ± 3.0	21.6 ± 2.7	22.8 ± 3.4
Heart rate (beats/min)	64 ± 9	64 ± 10	64 ± 8
Range (minimum–maximum)	43–80	43–80	52–78
Known extracardiac sarcoidosis	14 (58)	6 (43)	8 (80)
Known cardiac sarcoidosis	10 (42)	3 (21)	7 (70)
Cardiac signs and symptoms			
Syncope	9 (38)	4 (29)	5 (50)
Heart failure	6 (25)	1 (7)	5 (50)
Palpitations	3 (13)	1 (7)	2 (20)
Ventricular tachyarrhythmia	4 (17)	3 (21)	1 (10)
No signs and symptoms	5 (21)	5 (36)	0 (0)
Electrocardiographic data			
Advanced atrioventricular block	13 (54)	4 (29)	9 (90)
Atrial fibrillation	1 (4)	1 (7)	0 (0)
Implantable devices			
Pacemaker	8 (33)	0 (0)	8 (80)
Implantable cardioverter-defibrillator	2 (8)	0 (0)	2 (20)
Medications			
Beta-blockers	7 (29)	3 (21)	4 (40)
ACE-Is or ARBs	7 (29)	4 (29)	3 (30)
Diuretics	3 (13)	2 (14)	1 (10)
Amiodarone	3 (13)	2 (14)	1 (10)
Steroids	8 (33)	3 (21)	5 (50)
Echocardiographic results			
Left ventricular ejection fraction (%)	60 (44–65)	49 (43–61)	64 (54–73)
Presence of left ventricular wall thinning	13 (54)	9 (64)	4 (40)

Values are mean ± standard deviation, n (%), or median (interquartile range). ACE-Is = angiotensin-converting enzyme inhibitors; ARBs = angiotensin II receptor blockers.

Table 3. Distribution of hyperenhanced myocardium on DE-CT

Distribution	Overall (*n* = 24)
Presence of hyperenhancement	21 (88)
Multiple lesions	14 (58)
Transmurality	
Subendocardial	8 (33)
Midwall	5 (21)
Subepicardial	17 (71)
Transmural	14 (58)
Left ventricle	
Anterior wall	12 (50)
Septal wall	14 (58)
Inferior wall	15 (63)
Lateral wall	17 (71)

Values are *n* (%).

Table 4. Quantitative comparison between DE-CT attenuation and LGE-CMR signal intensity

	All patients (n = 24)	Without implantable devices (n = 14)	With implantable devices (n = 10)	p-value*
DE-CT attenuation (HU)				
Hyperenhanced myocardium	120 ± 16	117 ± 15	125 ± 17	0.28
Remote myocardium	77 ± 10	76 ± 12	77 ± 7	0.95
SD in remote myocardium	5.8 ± 1.6	5.8 ± 1.7	5.9 ± 1.5	0.95
Blood pool (left ventricular cavity)	114 ± 14	113 ± 16	117 ± 10	0.48
SNR for DE-CT	14.0 ± 4.0	14.2 ± 4.8	13.6 ± 2.7	0.72
CNR for DE-CT	8.1 ± 3.0	7.3 ± 2.5	9.2 ± 3.5	0.18
LGE-CMR signal intensity (SI)				
Hyperenhanced myocardium		1,341 ± 563	–	–
Remote myocardium		627 ± 323	–	–
SD in remote myocardium		107 ± 50	–	–
Blood pool (left ventricular cavity)		1,486 ± 450	–	–
SNR for LGE-CMR		7.0 ± 4.6	–	–
CNR for LGE-CMR		7.5 ± 3.2	–	–

Values are presented as mean ± standard deviation. SD = standard deviation, SNR = signal-to-noise ratio, CNR = contrast-to-noise ratio.

*p-values represent comparisons between patients with and without implantable devices.

Table 5. Comparison of DE-CT and LGE-CMR findings with clinical diagnosis for cardiac sarcoidosis.

DE-CT versus JSSOG criteria (n = 24)			
		DE-CT (Hyperenhanced myocardium)	
		Positive	Negative
JSSOG criteria	Positive	17	1
	Negative	4	2

LGE-CMR versus JSSOG criteria (n = 14)			
		LGE-CMR (Hyperenhanced myocardium)	
		Positive	Negative
JSSOG criteria	Positive	10	0
	Negative	3	1

Values are n. JSSOG = Japanese Society of Sarcoidosis and other Granulomatous Disorders.

Figure legends

Figure 1. Images for a 48-year-old woman with newly diagnosed cardiac sarcoidosis. Delayed contrast-enhanced CT using filtered back-projection (FBP, **a**) and knowledge-based iterative model reconstruction (IMR, **b**) and late gadolinium enhancement cardiac magnetic resonance (**c**) show focal hyperenhancement in the interventricular septum (*arrowheads*). The signal-to-noise ratios in the FBP and IMR images are 6.9 and 19.7, respectively. Note that image quality is better in IMR due to less noise.

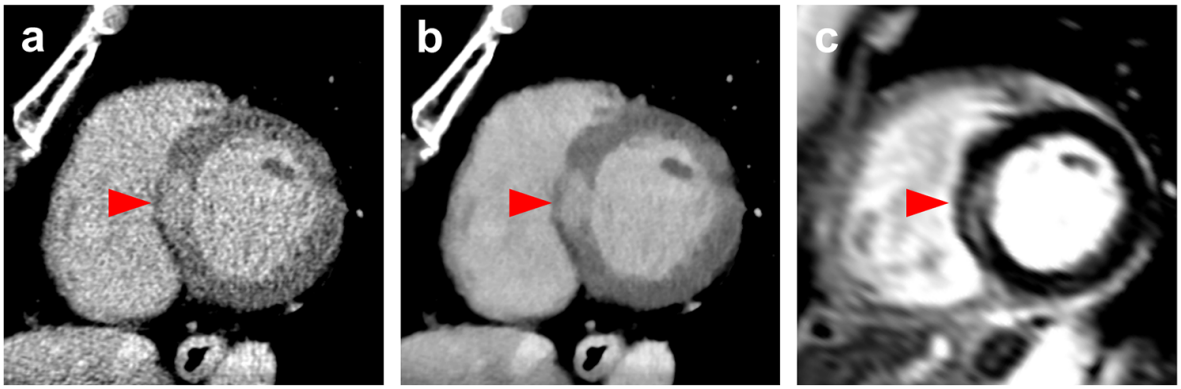

Figure 2. Images for a 71-year-old woman with newly diagnosed cardiac sarcoidosis. Echocardiography revealed a basal lateral wall aneurysm. Late gadolinium enhancement cardiac magnetic resonance (**a, c**) and delayed contrast-enhanced CT (**b, d**) show subepicardial distribution of hyperenhanced myocardium in the anterior to lateral and inferior wall. Yellow areas (**c, d**) denote myocardium ≥ 5 standard deviations above the mean for attenuation or signal intensity in the remote myocardium in the septum.

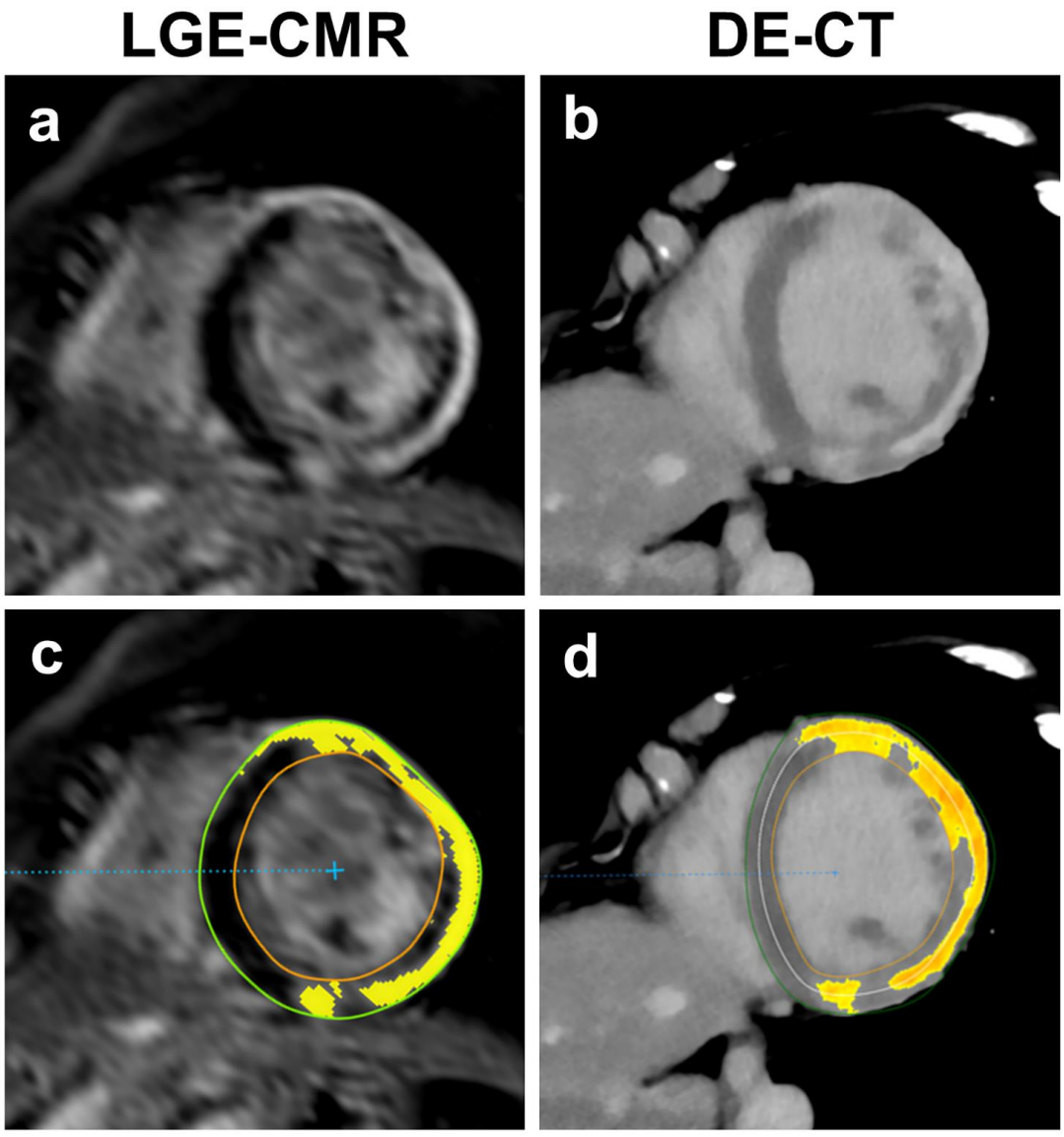

Figure 3. Delayed contrast-enhanced CT images for a 72-year-old woman with known cardiac sarcoidosis and an implantable cardioverter-defibrillator. (**a, b**) short axis view; (**c**) vertical long axis view. A varied distribution of hyperenhanced myocardium in the inferior to lateral wall (*arrowheads*) is clearly shown, even with artifacts from the implantable cardioverter-defibrillator. The reddish colour area (**b**) denotes myocardium 5–20 standard deviations above the mean for attenuation in the remote myocardium.

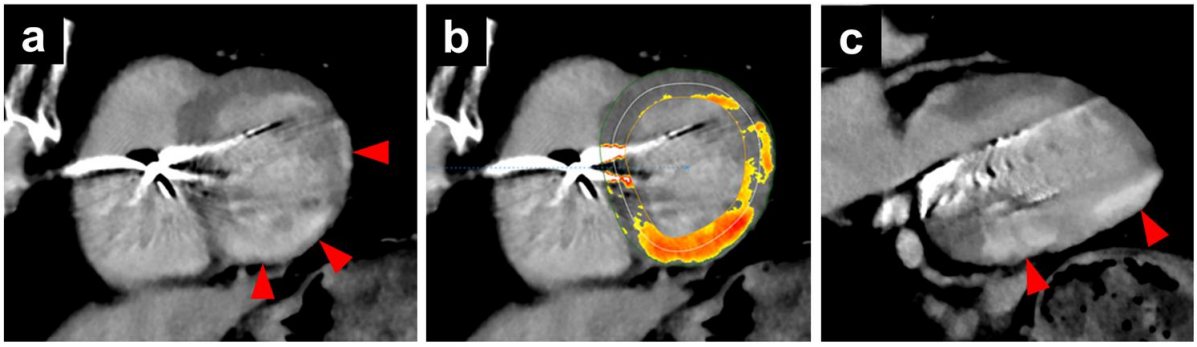

Figure 4. Scatter plots of correlation (**a, b**) and Bland-Altman analysis (**c, d**) for comparisons of the extent of hyperenhanced myocardium between delayed contrast-enhanced CT (DE-CT) and late gadolinium enhancement cardiac magnetic resonance (LGE-CMR) on a per-patient basis (**a, c**), and on a per-segment basis (**b, d**). CI = confidence interval, SD = standard deviation.